Modifying the Cu(111) Shockley surface state by Au alloying

Z. M. Abd El-Fattah,[1,2] M. Matena,[2] M. Corso,[2,3] M. Ormaza,[4] J. E. Ortega,[1,2,4] and F. Schiller[1,2]
[1]*Centro de Física de Materiales (CSIC-UPV-EHU) and Materials Physics Center (MPC), E-20018 San Sebastián, Spain*
[2]*Donostia International Physics Center, Paseo Manuel Lardizábal 4, E-20018 Donostia–San Sebastián, Spain*
[3]*IKERBASQUE, Basque Foundation for Science, E-48011 Bilbao, Spain*
[4]*Departamento de Física Aplicada I, Universidad del País Vasco, E-20018 San Sebastián, Spain*
(Received 9 October 2012; revised manuscript received 29 November 2012; published 17 December 2012)

The deposition of submonolayer amounts of Au onto Cu(111) results in a Au-Cu surface alloy with temperature- and thickness-dependent stoichiometry. Upon alloying, the characteristic Shockley state of Cu(111) is modified, shifting to 0.53 eV binding energy for a particular surface Au_2Cu concentration, which is a very high binding energy for a noble-metal surface. Based on a phase accumulation model analysis, we discuss how this unusually large shift is likely reflecting an effective increase in the topmost layer thickness of the order of, but smaller than, the value expected from the moiré undulation.

DOI: 10.1103/PhysRevB.86.245418 PACS number(s): 73.20.At, 73.61.At, 68.37.Ef

I. INTRODUCTION

Electronic states of (111)-oriented noble-metal surfaces have been a matter of research for a long time.[1–5] The reason is the presence of a textbooklike Shockley surface state inside a bulk-projected band gap at the center of the surface Brillouin zone. Being restricted to the outermost atomic surface layers, these surface states represent an almost ideal example of a two-dimensional electron gas on a metal surface. On the other hand, since both the structure and chemical composition of noble-metal surfaces can easily be modified, a variety of interactions and confinement effects can be studied through their surface states. The effect of impurities and defects has attracted a lot of interest due to the observation of standing-wave patterns in scanning tunneling microscopy and spectroscopy, which enable detailed surface science studies. Combinations of noble-metal surfaces in the form of overlayers,[6] alloys or compounds[7] revealed a notable influence on the Shockley state. One striking example is the Ag/Cu(111) monolayer system, which undergoes an irreversible phase transition from a moiré to a triangular dislocation network,[8] accompanied by the transformation of the surface state from a free-electron-like to a superlattice state.[9] Also, for physisorption, chemisorption, and even catalytic properties, the Shockley state of (111) noble metal surfaces is known to play an important role.[10]

In this work we will investigate the effect of Au adsorption on the Cu(111) surface state, as a function of both Au thickness and postannealing temperature. The thermal treatment eliminates three-dimensional growth and induces Au-Cu intermixing. The Au/Cu(111) alloyed system is a particularly useful template for fine-tuning the deeply structured superlattice state of Ag/Cu(111), so as to allow the observation of a Lifshitz transition.[11] For these purposes, we show that a small amount of Au and a mild annealing leads to the formation of a Au_2Cu surface alloy restricted to the outermost layer, with a characteristic Shockley-like surface state at 0.53 eV binding energy. This is an unexpectedly large binding energy that places the surface state away from the expected Cu(111)-Au(111) intermediate value. Based on the phase accumulation model in a quantum-well scenario, we discuss the nature of such a large energy shift with respect to Cu(111). We find that the topmost Au-Cu layer must feature an effective thickness increase, likely related to the moiré undulation that characterizes the Au-Cu surface alloy.

II. EXPERIMENT

Experiments were carried out at three different ultrahigh-vacuum systems. The photoemission data were taken in a home laboratory (San Sebastian) system using helium I ($h\nu = 21.2$ eV) light and at the Apple PGM beamline of the Synchrotron Radiation Center (SRC) of the University of Wisconsin in Stoughton (p-polarized light). In both cases a display-type hemispherical analyzer was used with angular and energy resolution set to 0.1° and 40 meV, respectively, for the angle-resolved measurements, versus ±7° and 70 meV resolution for the core-level experiments. The scanning tunneling microscopy (STM) experiments were carried out in San Sebastian using an Omicron VT Setup. The Cu(111) sample was cleaned by standard sputtering (800 V, 10^{-6} mbar Ne) and annealing (500 °C) cycles. Gold was deposited forming a wedge to allow a fast thickness-dependent characterization. The absolute thickness was monitored with a quartz microbalance and cross-checked with the Ag deposition on Cu(111), which produces well-split surface state peaks for one and two monolayers (ML) in the Ag/Cu(111) system.[8] The thickness indicated in the text is referred to a pure Au overlayer as in the Ag/Cu(111) system. The sample temperature during deposition was held at 120 K (SRC) and 180–300 K (San Sebastian).

III. RESULTS AND DISCUSSION

In Fig. 1 we show STM images taken for 0.3 ML Au deposited at room temperature and annealed to 350 °C. One observes two types of area, i.e., structureless patches with a few atomic protrusions and areas with a moiré-like pattern. The former are assigned to the clean copper substrate, featuring dispersed gold atoms, whereas the latter is attributed to a Au-Cu surface alloy formed during the annealing. The low-energy electron diffraction (LEED) showed no visible modification of the hexagonal Cu(111) pattern, by contrast to the superposition of Au(111) and Cu(111) diffraction patterns

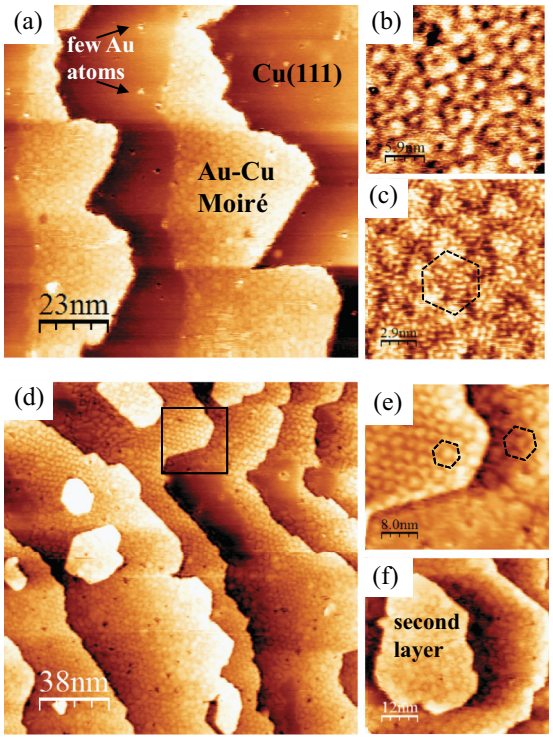

FIG. 1. (Color online) Large-scale STM images of (a) 0.3 ML (115×115 nm^2) and (d) 0.8 ML (190×190 nm^2) Au on Cu(111) annealed at 350 and 400 °C, respectively. (b), (c) and (e), (f) are zoomed areas of (a) and (d), respectively, revealing moiré-like structures. The hexagons mark the pseudohexagonal superlattice.

observed in non-annealed films. From the relative area covered by the moiré one can estimate a 60% Au concentration in the alloy, although a slightly different number can be deduced from the moiré periodicity, as discussed below. A closer look at the alloyed part [Figs. 1(b) and 1(c)] permits one to observe, at the atomic scale, a rather undefined corrugation, and at the nanoscale a pseudohexagonal superlattice with a ~3 nm lattice constant. In contrast to the Ag/Cu(111) system, the periodicity of the moiré-like reconstruction is difficult to define, due to its low topographic contrast and the odd rugosity at the atomic scale. These observations are similar to those reported earlier for this system.[12] At higher coverage, second-layer islands start to nucleate before covering the clean substrate completely. Higher annealing temperatures [e.g., 450 °C, Figs. 1(d)–1(f)] are needed to define a more homogeneous alloyed layer with a significant decrease of second-layer and clean substrate contributions. As shown in Figs. 1(d) to 1(f), higher annealing results in a better definition of the moiré pattern, although the superperiodicity is observed to vary from ~3 nm (in the middle of terraces and in second-layer islands) to ~5 nm (close to the lower parts of atomic steps). On the other hand, the random variation of moiré domains at a macroscopic (micrometer) scale, reflected in Fig. 1, explains the absence of moiré spots in the LEED pattern. In fact, a Fourier transform of Fig. 1(c) leads to a clear sixfold pattern, which is not present in the Fourier transform of large, micron-scale STM images.

At higher coverage and annealing temperatures the Cu surface appears homogeneously covered by the alloy and the clean surface reference is lost. The stoichiometry of alloyed areas can be crudely estimated from the periodicity of the moiré l_m, which is defined by the atomic registry of the overlayer with the substrate. For a two-dimensional Au_xCu_{1-x} surface alloy its atomic lattice constant a_x^s is, in a first approach,[13] the arithmetic average of the lattice constants of the growing metal (surface lattice constant $a_{Au}^s = 2.88$ Å) and the substrate ($a_{Cu}^s = 2.56$ Å):

$$a_x^s = x a_{Au}^s + (1-x) a_{Cu}^s. \quad (1)$$

Assuming that alloying takes place only at the outermost layer, the coincidence of substrate and overlayer lattices makes the moiré periodicity $l_m(x)$ stoichiometry dependent, as

$$l_m(x) = a_x^s \frac{a_{Cu}^s}{a_x^s - a_{Cu}^s}. \quad (2)$$

The moiré periodicity varies from $l_m = 32$ Å at 0.3 ML coverage and 350 °C annealing in Fig. 1(c) to $l_m = 32$–50 Å with 0.8 ML and 450 °C annealing in Fig. 1(e). From Eqs. (1) and (2) one obtains $x = 0.66$ for Fig. 1(c), and $x = 0.66$–0.5 for Fig. 1(e). The latter, which can be defined as a homogeneous 1 ML Au-Cu alloy with a Au_2Cu to AuCu stoichiometry, is the most interesting one from the surface state point of view, as will be discussed below.

In Fig. 2 we carry out a Au $4f$ core-level analysis intended to provide a deeper insight into the growth and alloying processes. In Fig. 2(a) we show some characteristic spectra taken at 125 eV photon energy and their data fits, whereas Fig. 2(b) shows the binding energy analysis focused on the Au $4f_{7/2}$ peak. At relatively low coverage (up to 0.2 ML) and low deposition temperature (120 K) one observes a spin-orbit-split peak at binding energies of 83.90 eV (Au $4f_{7/2}$) and 87.57 eV (Au $4f_{5/2}$). Both slightly increase by 30 meV from 0.2 ML to the nominal 1 ML coverage. The binding energy is similar to that for the non-alloyed 1 ML Au/Ru(0001) system ($E_B^{4f_{7/2}} = 83.88$ eV),[14] but different from that for the 1 ML Au/3 ML Cu/Ru(0001) interface ($E_B^{4f_{7/2}} = 83.99$ eV), where some alloying takes place at room-temperature deposition. Annealing the low-coverage Au/Cu(111) system (0.2 ML) leads to the alloy formation, as shown in the STM images of Fig. 1. This results in a strong, 240-meV-higher binding energy shift in both core levels ($E_B^{4f_{7/2}} = 84.14$ eV and $E_B^{4f_{5/2}} = 87.81$ eV), which does not depend on the annealing temperature. This is reflected in Fig. 2(b) for the Au $4f_{7/2}$ core level (points at low coverage). The binding energies are now similar to those for the annealed alloy-phase 1 ML Au/ 3 ML Cu /Ru(0001).[14] Notably, the total $4f$ area remains constant during annealing of the system at low coverage, indicating that Au is still at the surface, although in alloy form [low-coverage data in Fig. 2(c)].

The annealing of thicker Au films (above ~0.55 ML) has two main consequences in core-level positions: first, the appearance of a second contribution at the high-binding-energy side of the peak [Fig. 2(a)] and second, a significant upward shift of the main peak as a function of coverage for low annealing temperatures [Fig. 2(b)]. The higher-binding-energy emission is attributed to the presence of a second, subsurface alloyed layer, which gives rise to surface and bulk contributions in the $4f$ peak, as in pure Au. In contrast to the spectrum

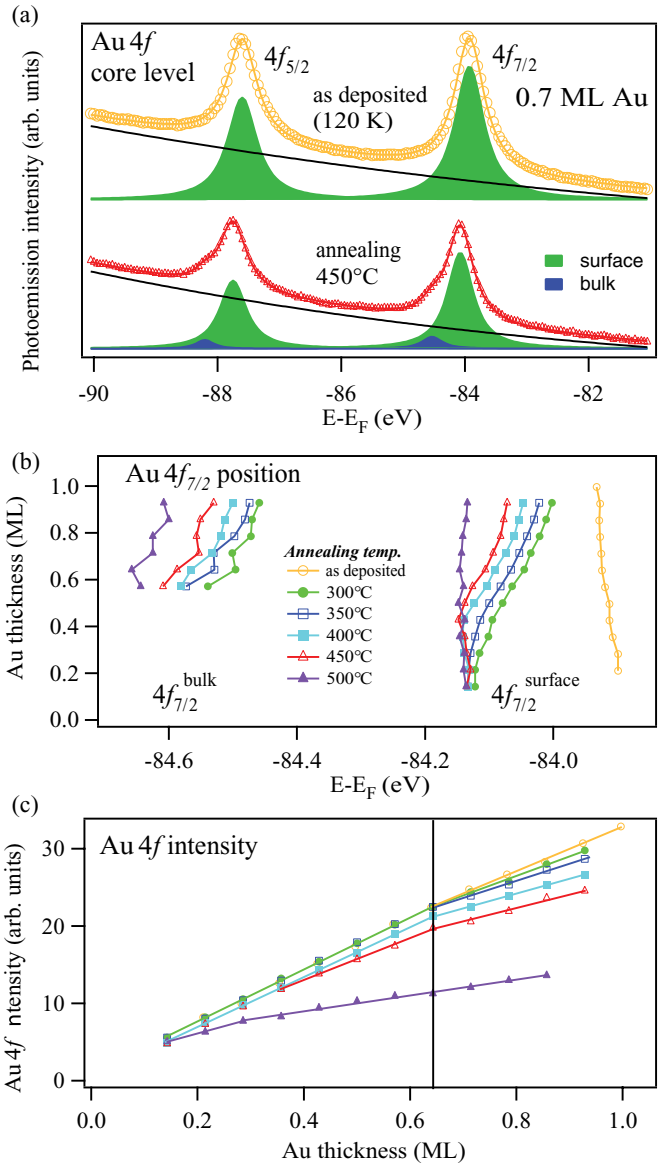

FIG. 2. (Color online) Au $4f$ core level as a function of Au thickness and annealing temperature: (a) 0.7 ML Au/Cu(111) spectra before and after annealing at 450 °C. The respective line fits (solid colored lines) are superimposed on the data (markers). (b) Positions of the Au $4f_{7/2}$ surface and bulk emissions, and (c) intensity of the total $4f$ contributions.

of the Au crystal, the subsurface bulk contribution in the present case is weaker than the surface one due to both the small amount of Au subsurface-layer contributions and the high surface sensitivity of the experiment. This involves 35 eV kinetic energy in Au $4f$ core-level electrons, i.e., close to the minimum of the electron escape depth.[15] Supporting the subsurface assignment of this shoulder, its intensity with respect to the surface peak increases at higher Au dosing. On the other hand, the upward shift with coverage observed at low annealing temperatures is attributed to insufficient alloying, i.e., a higher Au concentration that pushes the peak towards the binding energy of the low-temperature-deposited, non-alloyed films. The highest annealing temperature of 500 °C increases the Au atom mobility, leading to a homogeneous, well-formed Au-Cu alloy. Nonetheless, in Fig. 2(c) we observe a substantial decrease in the total Au $4f$ intensity at higher annealing temperatures. This is attributed to a deeper bulk alloying, beyond the subsurface.

All annealed samples (except the 500 °C one) reveal a small kink at approx. 0.65 ML Au coverage in the core-level intensity profile [Fig. 2(c)]. Above that coverage the Au $4f$ intensity increases at a lower speed. We assign this critical thickness to the completion of the first alloyed monolayer; additional Au atoms are incorporated in the subsurface and contribute less to the total core-level intensity due to the small electron escape depth. We estimate a maximum gold amount of 65% (core-level analysis) per layer, which agrees with the average 50%–66% Au concentration of the homogeneous 1 ML moiré that extends over the whole surface in the STM images.

The Shockley surface state of the Au/Cu(111) system also exhibit thickness and temperature dependence, which correlates well with the morphology and the core-level energy evolution, probed by STM and core-level photoemission. Angle-resolved photoemission spectra taken at room temperature and in normal emission (bottom of the surface band) are shown in Fig. 3. The deposition of small amounts of Au at low temperature (not shown) reveals a broader and weaker Cu(111) peak, as expected for a rougher Cu(111) surface. As shown in Fig. 3(a), a soft annealing up to 200 °C leads to the reappearance of a sharp Shockley state. For an increasing coverage, but still at low annealing temperatures ($T < 300$ °C), the surface state energy shifts back toward the Fermi level and the peak broadens. Such behavior is consistent with the presence of an inhomogeneous alloy, containing an increasing Au concentration, as deduced from the core-level analysis. Higher annealing temperatures that result in more homogeneous Au-Cu mixing lead to surface state sharpening and, more interestingly, to a noticeable higher-binding-energy shift. However the process saturates, i.e., excess coverage and excess annealing broadens the surface state peak and brings it back towards the Fermi energy. This can be observed across the different panels in Fig. 3. There is a maximum room-temperature binding energy ($E_B = 0.53$ eV), and a minimum linewidth (45 meV FWHM) for a critical coverage-temperature combination, namely, 0.65 ML Au and 450 °C annealing. In accordance with STM and Au $4f$ core-level analysis we attribute this surface state to the ideally sharp 1-ML-thick Au-Cu alloy, stoichiometrically close to $x \sim 0.65$. Deviations to higher or lower Au concentrations, as well as second-layer alloying, would shift and broaden the surface state.

Figure 4 displays the band dispersion and the Fermi surface of the 1 ML Au-Cu alloy with maximum surface state binding energy. No spin-orbit splitting, typical for the Au(111) surface state,[16] can be observed. The parabolic two-dimensional band produces the characteristic ringlike Fermi surface. The 300 K values for this Au-Cu alloy surface band are Fermi wave vector $k_F = 0.23$ Å^{-1}, and electron effective mass $m^* = 0.35m_e$. Its more interesting feature is the binding energy $E_B = 0.53$ eV, which is a very high value compared to other nobel-metal system. The band is then shifted by 140 meV from the Cu(111) substrate. Sizable downward shifts are typically observed in alkali-metal- or Al-covered Cu(111), but it is unusual for

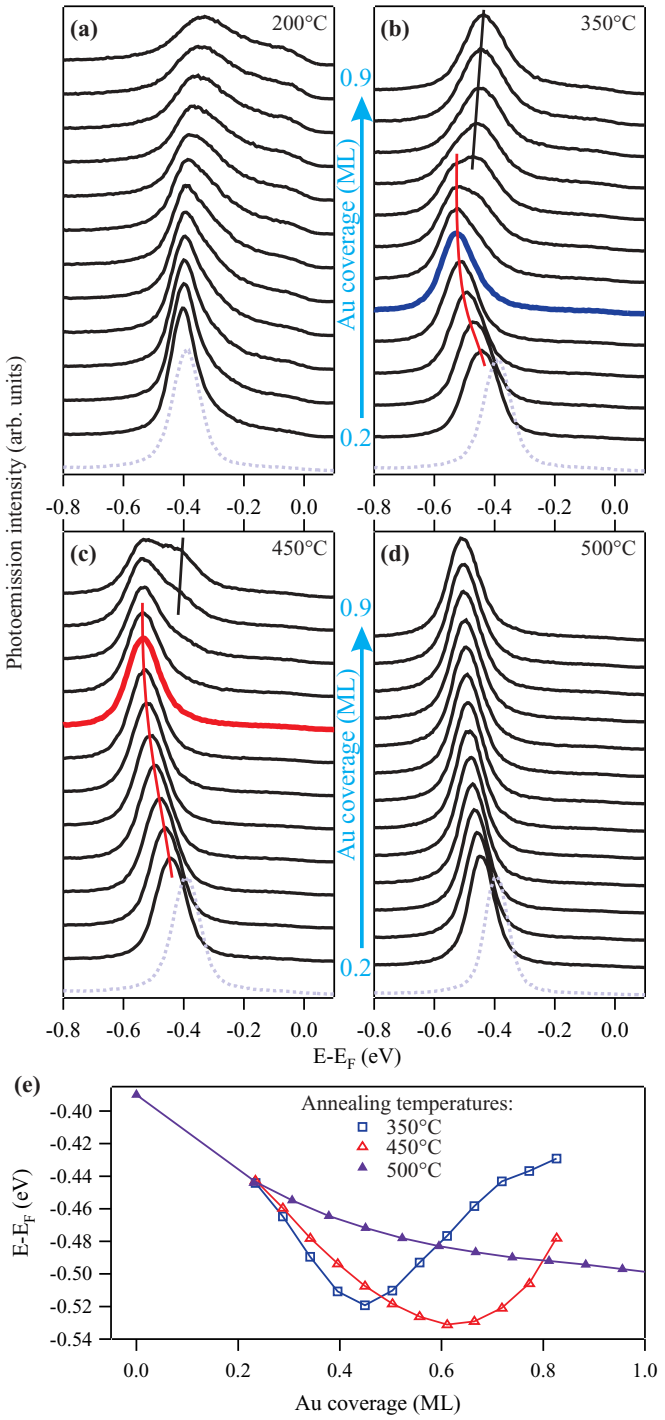

FIG. 3. (Color online) Evolution of the Shockley surface state for increasing coverages of Au on Cu(111), and postannealing to increasing temperatures from (a) to (d). The spectra correspond to the minimum of the surface band in each case. The highest binding energy found is marked in (b) and (c) with a different color. (e) Surface state energies from (b)–(d) plotted as a function of the Au thickness.

a noble-metal interface. At 300 K, the Shockley states for Cu(111) and Au(111) are respectively found at 0.39 and 0.44 eV below the Fermi energy.[4] Also the surface state in $Cu_3Au(111)$ is located close to the Cu(111) value of 0.39 eV at

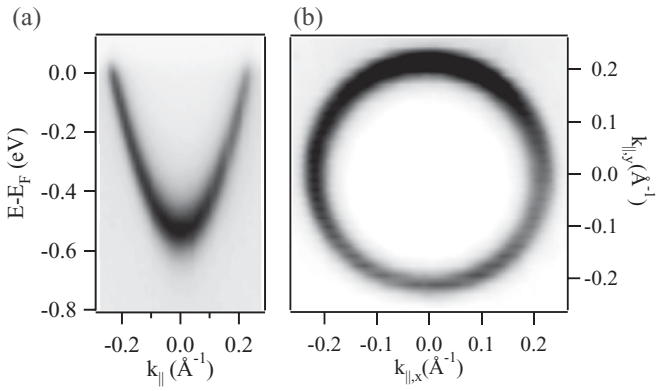

FIG. 4. (a) Surface state band for 0.65 ML Au/Cu(111) annealed at 450 °C, displayed as a photoemission intensity plot for $k_{\|,y} = 0$. (b) The corresponding two-dimensional Fermi surface.

300 K.[7] With respect to thin films deposited on (111)-oriented noble-metal surfaces, they smoothly evolve as a function of film thickness from the bare substrate energy to that of the growing material. A typical example is Ag/Au(111),[17,18] where the position of the surface state varies exponentially toward the Ag(111) surface state energy. In particular, for 1 ML Ag/Au(111) the binding energy is found halfway between those of surface states in Au(111) and Ag(111).

Therefore, the question arises of why the surface state of the 1 ML Au-Cu alloy lies at a high binding energy and out of the Au(111)–Cu(111) range. One important parameter is the position of the lower edge of the bulk-projected band gap (L_{4-} or $L_{2'}$ in single group notation) that supports the surface state. The band gap edge in our system shifts to higher binding energies from the Cu substrate to the 1 ML Au-Cu alloy by approx. 20 meV, therefore dragging the Shockley state along.[4] The $L_{2'}$ edge dependence of the surface state can be readily deduced from the phase accumulation model (PAM).[3] In the PAM, the surface state energies are calculated assuming constructive interferences of free-electron waves reflected back and forth at the crystal-vacuum interface, such that

$$\Phi_B + \Phi_C = 2\pi n. \tag{3}$$

Here Φ_C and Φ_B are the crystal and barrier phase changes, respectively, and n is an integer number with $n \geqslant 1$ for image and $n = 0$ for surface states.[3] The energy dependences of both Φ_C and Φ_B are given by the following expressions:[3,19]

$$\Phi_C = 2 \arcsin \sqrt{\frac{E - E_L}{E_U - E_L}} \tag{4}$$

and

$$\Phi_B = \pi \left(\sqrt{\frac{3.4\ \text{eV}}{E_V - E}} - 1 \right), \tag{5}$$

where E_L, E_U, and E_V are the lower and upper edges of the crystal bulk gap along ΓL and the vacuum energy, respectively. For an estimate of E_B in the 1 ML Au-Cu alloy, we may use Eqs. (3)–(5), together with the measured $E_L = 0.91$ eV band edge. Assuming $E_U = 4.25$ eV of Cu(111) and the measured

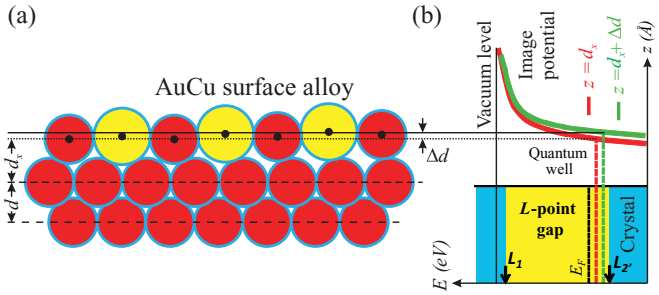

FIG. 5. (Color online) (a) Hard-ball model representation of the 1 ML Au-Cu/Cu(111) alloy system, indicating the positions of the successive Cu(111) planes. The effective corrugation of the topmost surface alloy Δd induces a phase shift of electron waves in the perpendicular direction, and hence a downward shift of the surface state with respect to Cu(111) (see the text). (b) Schematic representation of the potential in the vicinity of the flat and alloyed surface shown in (a).

value $E_V = 5.3$ eV, we obtain an upward binding energy shift of 90 meV, in contrast to the downward 140 meV shift observed.

Note that the 1 ML Au-Cu alloy exhibits both structure and composition at variance with those of the Cu(111) substrate. Such structural variations are not accounted for in the surface state scenario of Eq. (3). The presence of the structurally different outermost surface layer can be conveniently rationalized by considering it a separate quantum well of size d^*, as sketched in Fig. 5. The alloy quantum well can be treated, within the same PAM approach, by adding a phase shift Φ^* to Eq. (3),[20,21] where $\Phi^* = 2k_\perp d^*$ is a consequence of the optical path traveled by the electron wave inside the monolayer alloy in a complete vacuum-to-Cu-crystal round trip:

$$\Phi_B + \Phi_C + 2k_\perp d^* = 2\pi n, \tag{6}$$

where Φ_C is that of the pure Cu crystal, $k_\perp$ stands for an electron momentum perpendicular to the surface,[20,22] and $d^* = d_x + \Delta d$ is the physical thickness of the Au-Cu alloy layer, namely, the interplanar distance $d_x = a_x/\sqrt{3}$ plus any effective surface corrugation Δd, e.g., that of the moiré. a_x can be assumed to be the lattice constant of the Au_2Cu compound, such that Eq. (1) gives $a_x = 3.92$ Å and $d_x = 2.26$ Å.

For Shockley-like surface states $k_\perp$ equals the fundamental π/d_x wave vector. Solving Eq. (6) for the 1 ML alloy surface state energy ($E_B = 0.53$ eV) and $k_\perp = \pi/d_x$, one obtains $\Delta d = 0.085$ Å. This value is lower than the average rugosity provoked by the moiré undulation. The latter can be assumed as half of the top-to-hollow height difference, which for pure Cu(111) gives $\Delta d_{\text{moiré}} = 0.23$ Å. The deviation from Δd could suggest a vertical effective relaxation of the moiré, which is not detectable by regular LEED or STM, or simply reflect the limits of the PAM approach. In reality the wave number $k_\perp$ in Eq. (6) is ill defined. As discussed for the Pd/Cu(111) system,[21] $k_\perp$ is equal to or lower than π/d_x, depending on whether the surface state lies, respectively, above (pure surface state) or below (quantum well state) the L_2' edge of the corresponding Au_2Cu bulk band gap. In fact, a small 6% reduction from π/d_x makes $\Delta d = \Delta d_{\text{moiré}}$. However, the Au_2Cu bulk band structure is unknown, and hence such a reduction in the effective $k_\perp$ cannot be ascertained.

IV. CONCLUSIONS

Au deposition on Cu(111) results in a surface alloy whose morphology and Au-Cu stoichiometry depend on the amount of Au added to the system and the postannealing temperature. The thickness and temperature dependence is also observed in the characteristic Shockley surface state. For 0.65 ML and 450 °C we obtain a homogenous, 1-ML-thick Au-Cu alloy that exhibits an unexpectedly large surface state binding energy, larger than that of Au(111). Based on the phase accumulation model, and assuming a Au-Cu monolayer-thick quantum well, we discuss the large surface state energy, and attribute it to an effective increase in the topmost layer thickness.

ACKNOWLEDGMENTS

This work was supported in part by the Spanish MINECO (Grants No. MAT2010-21156-C03-01 and No. MAT2010-21156-C03-03), and the Basque Government (Grant No. IT-257-07). The SRC is funded by the National Science Foundation (Award No. DMR-0084402).

[1] W. Shockley, Phys. Rev. **56**, 317 (1939).
[2] S. D. Kevan, N. G. Stoffel, and N. V. Smith, Phys. Rev. B **31**, 3348 (1985).
[3] N. V. Smith, Phys. Rev. B **32**, 3549 (1985).
[4] R. Paniago, R. Matzdorf, G. Meister, and A. Goldmann, Surf. Sci. **336**, 113 (1995).
[5] F. Reinert, G. Nicolay, S. Schmidt, D. Ehm, and S. Hüfner, Phys. Rev. B **63**, 115415 (2001).
[6] T.-C. Chiang, Surf. Sci. Rep. **39**, 181 (2000).
[7] R. Courths, M. Lau, T. Scheunemann, H. Gollisch, and R. Feder, Phys. Rev. B **63**, 195110 (2001).
[8] A. Bendounan, H. Cercellier, Y. Fagot-Revurat, B. Kierren, V. Y. Yurov, and D. Malterre, Phys. Rev. B **67**, 165412 (2003).
[9] F. Schiller, J. Cordón, D. Vyalikh, A. Rubio, and J. E. Ortega, Phys. Rev. Lett. **94**, 016103 (2005).
[10] F. Forster, A. Bendounan, J. Ziroff, and F. Reinert, Phys. Rev. B **78**, 161408 (2008).
[11] Z. M. Abd El-Fattah, M. Matena, M. Corso, F. J. García de Abajo, F. Schiller, and J. E. Ortega, Phys. Rev. Lett. **107**, 066803 (2011).
[12] J. Jia, Y. Hasegawa, K. Inoue, W. S. Yang, and T. Sakurai, Appl. Phys. A: Mater. Sci. Process. **66**, S1125 (1998).
[13] L. Vegard, Z. Phys. **5**, 17 (1925).
[14] M. Kuhn, A. Bzowski, T. Sham, J. Rodriguez, and J. Hrbek, Thin Solid Films **283**, 209 (1996).
[15] W. A. Dench and M. P. Seah, Surf. Interface Anal. **1**, 1 (1979).
[16] S. LaShell, B. A. McDougall, and E. Jensen, Phys. Rev. Lett. **77**, 3419 (1996).

[17]H. Cercellier, C. Didiot, Y. Fagot-Revurat, B. Kierren, L. Moreau, D. Malterre, and F. Reinert, Phys. Rev. B **73**, 195413 (2006).
[18]C.-M. Cheng, K.-D. Tsuei, C.-T. Tsai, and D.-A. Luh, Appl. Phys. Lett. **92**, 163102 (2008).
[19]F. Schiller, M. Heber, V. D. P. Servedio, and C. Laubschat, Phys. Rev. B **70**, 125106 (2004).
[20]J. E. Ortega and F. J. Himpsel, Phys. Rev. Lett. **69**, 844 (1992).
[21]Y. Hasegawa, T. Suzuki, and T. Sakurai, Surf. Sci. **514**, 84 (2002).
[22]M. A. Mueller, A. Samsavar, T. Miller, and T.-C. Chiang, Phys. Rev. B **40**, 5845 (1989).